Journal of Peptide Science
J. Peptide Sci. **10**: 666–677 (2004)
Published online 10 June 2004 in Wiley InterScience (www.interscience.wiley.com). DOI: 10.1002/psc.582

JOURNAL OF PEPTIDE SCIENCE

First Chemical Synthesis of a Scorpion α-Toxin Affecting Sodium Channels: The Aah I Toxin of *Androctonus Australis Hector*

SARRAH M'BAREK,[1] ZIAD FAJLOUN,[1,2] SANDRINE CESTÈLE,[1,3] CHRISTIANE DEVAUX,[1] PASCAL MANSUELLE,[1] AMOR MOSBAH,[1,2] BESMA JOUIROU,[1,4] MASSIMO MANTEGAZZA,[3] JURPHAAS VAN RIETSCHOTEN,[1] MOHAMED EL AYEB,[4] HERVÉ ROCHAT,[1] JEAN-MARC SABATIER[1,2] and FRANÇOIS SAMPIERI[1]*

[1] FRE 2738 CNRS-Université de la Méditerranée, Laboratoire de Biochimie and Laboratoire International Associé d'Ingénierie Biomoléculaire, IFR Jean Roche, Faculté de Médecine Nord, Bd Pierre Dramard, 13916 Marseille Cedex 20, France
[2] Laboratoire Cellpep SA, 13–15 Rue Ledru-Rollin, 13015 Marseille, France
[3] Laboratorio di Neurofisiologia, Istituto Neurologicao Besta (Bicocca), Via Temolo 4, 20125 Milano, Italia
[4] Laboratoire des venins et toxines, Institut Pasteur de Tunis, P.O. Box 74, 1002 Belvédère, Tunis, Tunisia

Received 19 December 2003
Revised 16 January 2004
Accepted 6 February 2004

Abstract: Aah I is a 63-residue α-toxin isolated from the venom of the *Buthidae* scorpion *Androctonus australis hector*, which is considered to be the most dangerous species. We report here the first chemical synthesis of Aah I by the solid-phase method, using a Fmoc strategy. The synthetic toxin I (sAah I) was renatured in DMSO-Tris buffer, purified and subjected to thorough analysis and comparison with the natural toxin. The sAah I showed physico-chemical (CD spectrum, molecular mass, HPLC elution), biochemical (amino-acid composition, sequence), immunochemical and pharmacological properties similar to those of the natural toxin. The synthetic toxin was recognized by a conformation-dependent monoclonal anti-Aah I antibody, with an IC_{50} value close to that for the natural toxin. Following intracerebroventricular injection, the synthetic and the natural toxins were similarly lethal to mice. In voltage-clamp experiments, $Na_v1.2$ sodium channel inactivation was inhibited by the application of sAah I or of the natural toxin in a similar way. This work describes a simple protocol for the chemical synthesis of a scorpion α-toxin, making it possible to produce structural analogues in time.

Keywords: scorpion α-toxin; Aah I; solid-phase peptide synthesis; sodium channel; oxidation/refolding

Abbreviations: 3D, three-dimensional; Aah I, Aah II, Aah III, toxin I, toxin II and toxin IIII, respectively, from the scorpion *Androctonus australis hector*; Ab, mAb, pAb, antibody, monoclonal or polyclonal antibody, respectively; Abu 8 Aah I, synthetic Aah I derivative with 1/2 cystines replaced by aminobutyric acid; BSA, bovine serum albumin; DMF, dimethylformamide; Fmoc, N^{α}-(9-fluorenyl)methyloxycarbonyl; HMP, 4-hydroxy-methylphenyloxy; i.c.v., intracerebroventricular; IC_{50}, concentration giving half-maximal inhibition; IgG, immunoglobulin G; K_d, thermodynamic dissociation constant; LD_{50}, 50% lethal dose; MALDI-TOF, matrix-assisted laser desorption ionisation-time of flight; MS, mass spectrometry; nAah I or sAah I, natural or synthetic Aah I toxin, respectively; NaCh(s), voltage-gated sodium channel(s); NMP, *N*-methyl pyrrolidone; PBS, phosphate buffer saline; RP-HPLC, reverse-phase high-performance liquid chromatography; SDS, sodium dodecyl sulphate; Ts 7, toxin 7 from the scorpion *Tityus serrulatus*.

*Correspondence to: François Sampieri, Laboratoire de Biochimie CNRS UMR 6560, and Laboratoire International Associé d'Ingénierie Biomoléculaire, IFR Jean Roche, Faculté de Médecine Nord, Bd Pierre Dramard, 13 916, Marseille Cedex 20, France; e-mail: sampieri.f@jean-roche.univ-mrs.fr
Contract/grant sponsor: French CNRS.
Contract/grant sponsor: Université de la Méditerranée.
Contract/grant sponsor: Cellpep S.A.

INTRODUCTION

Scorpion stings are a worldwide public health concern and, in many cases, scorpion envenomation leads to a neurotoxic syndrome, known as scorpionism syndrome [1,2], which may result in the death of the patient in 1–3% of cases. The acute toxicity of *Buthidae* scorpion venoms is due to very low amounts of extremely potent neurotoxic polypeptides (neurotoxins) [3] that selectively affect voltage-gated Na^+-channels (NaCh) of excitable cells. Scorpion venoms also contain K^+-channel-selective neurotoxins that block trans-membrane K^+ currents but do not induce noticeable neurotoxic effects by peripheral injection [4,5].

In the three last decades, many Na^+-channel-selective neurotoxins have been isolated and characterized from scorpion venoms [6,7]. They constitute a rich and well studied group of mostly basic, small, packed proteins, consisting of a single chain of 60–76 residues cross-linked by four disulphide bridges. These so-called 'long-chain' scorpion neurotoxins have to be distinguished from the 'short-chain' group of K^+-channel-selective scorpion neurotoxins.

Most of the Na^+-channel-selective scorpion neurotoxins are species-selective, i.e. they may affect either mammals, insects (excitatory [8,9] or depressant [10,11] insect-selective toxins), or crustaceans exclusively [12,13], whereas only a few others are toxic to both mammals and insects [14–17]. Their remarkable biological effects on mammals or insects result from interference with the action potential of excitable cells. Two subclasses of toxins that showed to affect either inactivation (α-type toxins) or activation (β-type toxins) of voltage-gated NaChs have been distinguished [18,19]. In the 10 last years, however, some variations in the above classification have emerged [7]. Thus, α-like toxins were distinguished from genuine α-toxins, based on pharmacological specificity revealing a putative new brain NaCh subtype [20,21]. Alpha-scorpion toxins were the first to be isolated and characterized in scorpion venoms [3,22]. They strongly affect the inactivation of voltage-gated NaChs [6,19,23] by binding to the so-call 'site 3' [24,25], which consists in the IVS3-S4 loop and part of the I/IVS5-S6 extra-cellular loop at the channel surface [25,26].

During the two last decades, 3D structures of diverse NaCh-selective scorpion neurotoxins have been experimentally obtained. Crustacean-selective, as well as α-, α-like and β-type mammal-selective toxins, all showed similar folding/disulphide-pairings and secondary structure patterns (an α-helix linked to a triple-stranded β-sheet by two disulphide bridges) [13,27–31], but excitatory insect-selective toxins exhibited a different disulphide pairing and an additional α-helix [32]. Structure-function of NaCh-scorpion toxins has been studied since the 1970s. In the earliest works [33–35], as well as more recently [36], reactive residues of a few relevant toxins were chemically modified to study correlation with possible changes in biological activity. These structural and functional studies were possible only since the toxins had been purified on a large scale [37]. However, scorpion venoms are generally difficult to collect and their toxin content is very low. Two methods have contributed to overcome the scarcity and high cost of natural toxins: recombinant expression systems and chemical synthesis. The first method led to a number of successes: the insecticidal toxin LqhαIT was produced, by recombinant expression in bacteria, as the natural molecule and engineered mutants, for identifying residues important for activity [38,39]. The excitatory insect-selective toxin Bj-xtrIT and selected mutants were expressed in the same system for 3D structure determination [32] and functional analyses [40]. The mammal-selective α-like toxin BmK M1 was expressed in yeast and showed the same activity as the natural toxin [41], while recombinant variants with mutated half-cystines were produced recently for deciphering the role of disulphides in its activity [42]. It seems, however, that the success in producing long toxins by recombinant expression relies on their favourable physico-chemical properties and also on the tolerance of the biological expression system towards the produced molecules. Thus, even if the mammal-selective Aah II and insect-selective Aah IT1 toxins were produced as fully bioactive molecules in cultured cells or in yeast, yields were very low [43,44]. In such difficult cases, chemical synthesis may be considered as an alternative to recombinant expression. Besides, the chemical technique offers the possibility of making mutants with unusual residues [45,46]. Many successful chemical syntheses of short (30–40 residues) scorpion neurotoxins affecting potassium channels have been reported [47–52], but, until now, chemical synthesis of long-chain toxins have proved to be more difficult to succeed in uniting the assembly of the complete polypeptide chain with correct oxidation and folding [53,54].

We report here the successful chemical synthesis of a long-chain α-scorpion neurotoxin, the toxin

I of *Androctonus australis hector* (Aah I), by standard methods. We obtained enough synthetic toxin for ascertain that its physicochemical and biological properties are very similar to those of the natural toxin.

MATERIALS AND METHODS

Materials

Natural Aah I toxin (nAah I) was purified, in our laboratory, from the venom of the scorpion *Androctonus australis hector*, by Dr Martin-Eauclaire [37]. N^{α}-(9-fluorenyl)methyloxycarbonyl-L-amino acid (Fmoc-amino acid) derivatives, 4-hydroxymethylphenoxy (HMP) resin and the reagents used for peptide synthesis were purchased from Perkin-Elmer. Solvents were analytical grade products from SdS company (Peypin, France). α-Cyano-4-hydroxycinnamic acid was obtained from Sigma (St Louis, MO, USA).

Methods

Chemical synthesis of sAah I. The synthetic Aah I (sAah I) was obtained by the solid-phase technique [55], using a Fmoc strategy on an automated peptide synthesizer (Model 433A, Applied Biosystems, Foster City, CA, USA). The side chain-protecting groups used for trifunctional residues were: trityl for Cys, His and Asn; tert-butyl for Ser, Thr, Tyr and Asp; pentamethylchroman for Arg, and tert-butyloxycarbonyl for Lys and Trp.

At first, 1.0 mmol of Fmoc-threonine was activated with 0.5 mmol of N,N′-dicyclohexylcarbodiimide [0.5 ml of 1 M solution in dimethylformamide (DMF)], in presence of 0.22 mmol of 4-dimethylaminopyridine [2.2 ml of 0.1 M solution in *N*-methylpyrrolidone (NMP)], and coupled to 0.3 mmol (0.273 g) of 1.1 mmol/g-functionalized 'Wang' HMP resin [56]. Residual free hydroxyl functional groups were blocked by percolating the Fmoc-threonine-coupled resin with 1.0 mmol of benzoic anhydride dissolved in 2.1 ml NMP, according to Sieber [57]. For the following steps, *N*-α-amino groups were deprotected by treatment with piperidine diluted in NMP (18 and 20%, v/v), for 3 and 8 min, respectively. Then, the peptidyl-resin was washed several times with NMP (5×1 min) and the Fmoc-amino acid derivatives (1 mmol, 3.3-fold excess) were coupled (20 min) as their hydroxybenzotriazole active esters, obtained after activation with equimolar amounts (1.0 mmol) of 2-(1H-benzotriazol-1-yl)-1,1,3,3-tetramethyluronium hexafluorophosphate, 1-hydroxybenzotriazole, and *N,N*-diisopropylethylamine, in solution in 2.5 ml of a NMP/DMF (1 : 5 v/v) mixture.

After peptide chain assembly was completed and the N-terminal Fmoc group removed, the final peptidyl-resin was thoroughly desiccated and weighed. About 1.8 g of peptidyl-resin was treated, with stirring, for 2.5 h at room temperature, with a mixture of trifluoroacetic acid (TFA)/H_2O/thioanisole/ethanedithiol (88 : 5 : 5:2, v/v) in the presence of crystalline phenol (2.25 g) in a final volume of 30 ml/g of peptidyl-resin. The peptide-resin mixture was filtered to remove the resin, and the filtrate was precipitated and washed three times in cold di-ethyl oxide. The resulting crude peptide was pelleted by centrifugation (3000 *g*; 10 min) and the supernatant was discarded. The final crude peptide (about 690 mg) was dissolved in H_2O and freezedried.

Oxidation/folding and physicochemical characterization of sAah I. Two experiments of sAah I oxidation/folding were performed at two peptide concentrations. One of both gave the best final yield, whereas the other furnished most of the synthetic product to be used for analytical experiments and biological tests. Two batches of the crude synthetic peptide: A (40 mg, 5.88 μmol) and B (25 mg, 3.67 μmol) were each dissolved in 4.0 ml of a solution of DMSO/H_2O (1 : 1, v/v). Then, 1.0 ml of 0.2 M Tris–HCl buffer, pH 8.3 was added to give a final peptide concentration of 1.18 mM (batch A) or 0.73 mM (batch B) in 5 ml. The mixtures were stirred under air to allow folding to occur at room temperature. Samples of 200 μl of batch A were taken at several times for analysis by reverse phase HPLC and mass spectrometry. After about 72 h of refolding, a conspicuous precipitate formed in both experiments. We therefore filtered the peptide solutions through a 0.2 μm filter, then the filtrates were stirred under air for a further 88 h, giving a total time of 160 h. The target products were both purified to homogeneity by semi-preparative reverse-phase (RP) HPLC (Perkin-Elmer, C_{18} Aquapore ODS 20 μm, 250×10 mm column), using a 60 min linear gradient from 0 to 40% of buffer B [0.08% (v/v) TFA-acetonitrile] in buffer A [0.1% (v/v) TFA/H_2O], at a flow rate of 5 ml/min ($\lambda = 230$ nm). The eluates were fractionated according to their UV absorbance, then fractions were analysed by matrix-assisted laser desorption ionisation-time of flight

mass spectrometry (MALDI-TOF MS) and only those fractions that showed the synthetic toxin without contaminants were pooled and freeze-dried.

The homogeneity and identity of sAah I from batch A were assessed by: (i) analytical HPLC (Merck Chromolith RP18, 5 μm, 100 × 4.6 mm column), using a 40 min linear gradient from 0 to 60% of buffer B [0.08% (v/v) TFA-acetonitrile] in buffer A [0.1% (v/v) TFA/H_2O] at a flow rate of 1 ml/min ($\lambda = 230$ nm); (ii) co-elution of 4.5 nmol of sAah I with 4.5 nmol of natural Aah I, in the same conditions as for (i), but using a 60 min linear gradient from 0 to 60% of the same buffers; (iii) amino-acid analyses after hydrolysis [6 N HCl/2% phenol (w/v), 20 h, 110 °C, under low pressure of nitrogen]; (iv) mass determination by MALDI-TOF MS; (v) Edman sequencing of 500 pmol of S-carboxamidomethylated sAah I (from batch B) on an Applied Biosystems 476A sequencer, using the recommended program, unless a proline residue was expected, in which case the coupling temperature was increased from 48 to 50 °C and the cleavage time from 5 to 10 min. Peptide deletion was estimated by quantifying the amino-acid preview [58] on stable and reliable PTH derivatives.

CD spectra. Samples of natural and synthetic Aah I (from batch B) were submitted to circular dichroism spectrometry. The concentrations of AahI or sAahI in the samples (0.1 mg/ml) were assessed by amino acid analyses. The CD spectra were recorded on a Jasco J-800 Dichrograph. A ratio of 2.20 was found between the positive CD band at 290.5 nm and the negative band at 192.5 nm. CD spectra were reported as the absorption coefficient ($\Delta\varepsilon$) per amide. The far UV CD spectra were acquired at 20 °C in H_2O between 190 and 260 nm using 0.1 cm path length cell. Data were collected twice at 0.5 nm intervals with a scan rate of 50 nm/min.

Biological Assays

Immunoassays. The production of monoclonal anti-Aah I antibodies (mAb 9C2) was previously described [59]. IgG from hybridoma 9C2 (IgG2a, κ) was obtained by purification on protein A-Sepharose (Amersham Pharmacia Biotech, France) followed by dialysis in borate-buffered saline, pH 7.9. The production of polyclonal anti-Aah I antibodies (pAb P111) was previously described [60].

The immunoreactivity of natural and synthetic Aah I was tested in liquid-phase RIA, in which we assessed the ability of each toxin to inhibit the binding of [^{125}I]-Aah I to mAb 9C2 or pAb P111. Toxin Aah I (0.5 nmol) was radiolabelled with iodine-125 (Amersham) by the lactoperoxidase method and was purified as described by Rochat *et al.* [61]. All assays were performed in duplicate. For competitive RIA experiments, 25 μl of IgG 9C2 (2×10^{-10} M) or IgG P111 (2.5×10^{-5} M) was mixed with 25 μl of [^{125}I]-labelled Aah I (0.4×10^{-10} M) in the presence of a series of dilutions of unlabelled natural or synthetic toxin. We used IgG dilutions giving approximately 40% of the maximum possible binding. The mixtures were incubated for 90 min at 37 °C, then overnight at 4 °C. Sheep anti-mouse (for mAb) or anti-rabbit (for pAb) precipitating antibodies (0.5 ml; UCB Bioreagents, Valbiotech, France) were added. The mixtures were incubated for 30 min at 4 °C, and immune complexes were pelleted by centrifugation at 9000*g* for 20 min. The radioactivity of the pellets was measured with a gamma-ray counter (RIAS-TAR, Packard). Results are expressed as B/B_0, where B and B_0 are the radioactivity bound to antibodies in the presence (B) or absence (B_0) of unlabelled ligand.

Assay for in vivo toxicity of natural and synthetic Aah I in mice. We determined the toxicity of natural and synthetic Aah I *in vivo* by determining the 50% lethal does (LD_{50}) after intracerebroventricular (i.c.v.) injection into 20 g female C57BL/6 mice. We injected 5 μl of various concentrations of the toxin in PBS containing 0.1% (w/v) BSA into groups of six mice per dose tested. The number of surviving mice was recorded 24 h after injection. The LD_{50} was calculated according to Behrens and Karber [62]. Mice were housed in the conventional facilities of the laboratory. Animal housing and experiments were carried out in accordance with European guidelines (no. 86/609/CEE) on animal welfare.

Electrophysiological recordings. We maintained tsA201 cells at 37 °C under a 5% CO_2 atmosphere in DMEM/F12 medium (GIBCO/BRL/Life Technologies) supplemented with 10% bovine serum (GIBCO/BRL/Life Technologies), 20 μg/ml penicillin and 10 μg streptomycin (Sigma). We transiently co-transfected tsA-201 cells with cDNAs by using the pCDM8 vector for the channel α-subunit, and the EYFPO-N1 vector encoding the enhanced yellow fluorescent protein (Clontech), using the calcium phosphate precipitation method [63]. Successfully transfected cells were identified on the basis of their yellow fluorescence.

Whole-cell sodium currents were recorded in tsA-201 cells expressing Na_v 1.2 NaChs, 24–36 h

after transfection. Experiments were conducted at room temperature. The external recording solution consisted of 150 mM NaCl, 10 mM CsHepes, 1 mM $MgCl_2$, 2 mM KCl and 1.5 mM $CaCl_2$ (pH = 7.4). The internal recording solution consisted of 105 mM CsF, 10 mM Hepes, 35 mM NaCl, 10 mM EGTA (pH = 7.4). Electrode resistances were typically 1.5–2.5 MΩ in the bath. Recordings were obtained with an Axopatch 1D patch-clamp amplifier (Axon Instruments). Voltage pulses were applied and data were acquired with pClamp 8 software (Axon Instruments) and analysed with Origin 6 (Microcal). Linear leak and capacitance currents were subtracted using an on-line P/4 subtraction paradigm. Both natural and synthetic Aah I were dissolved in the extracellular recording solution, at the final concentration indicated, and applied directly to the cells.

RESULTS

Chemical Synthesis of sAah I

The amino-acid sequence of Aah I [64] is shown in Fig. 1, aligned with the sequences of Aah II and Aah III, two structurally related long-chain scorpion toxins. Aah I shares 42% sequence identity with Aah II [65], and 78% with Aah III [66], both of which are also found in the venom of *Androctonus australis hector*. Contrary to Aah II, the Aah I toxin has its C-terminal carboxyl group free, hence the use of the benzyl alcohol-type resin. After stepwise assembly of the peptide on 0.3 mmol HMP resin and removal of the last Fmoc protecting group, the mass increase of the resin, i.e. approximately the mass of the side-chain-protected peptide, was about 3.1 g, which represents about 86% of the expected mass increase (3.62 g, calculated from a theoretical molecular mass of 12 075.3 Da for the side-chain-protected peptide). After acidolysis of a sample of 1.8 g of peptidyl resin, the mass of the crude deprotected Aah I peptide was 690 mg (74% of the expected mass). Figure 2(a) shows the elution profile, on analytical C_{18} reverse-phase HPLC, of a sample of the crude peptide. Its MALDI-TOF mass spectrum (not shown) showed that it contained reduced Aah I, but also deleted and truncated peptides.

Two separate experiments of folding/oxidation of the crude peptide were carried out in concentrated (batch A, 1.17 mM) and less concentrated (batch B, 0.73 mM) synthetic toxin conditions (see experimental procedures). In both experiments, a precipitate progressively occurred. It was filtered out at about the middle of the oxidation course. The precipitate was partially soluble in pure DMSO and was shown by MS to be composed of a few species of strongly deleted or truncated peptides in the 2000–4000 Da range, but also of minor amounts of partially oxidized toxin (not shown). No further precipitation occurred during the second period of oxidation of the soluble filtrate. At the end of the reaction, 200 µl of the batch A medium were submitted to analytical reverse-phase HPLC. The elution profile [Fig. 2(b)] shows a narrow peak that eluted at 26.7 min and corresponds to completely oxidized sAah I, as assessed by MALDI-TOF (not shown). The remainder of oxidized batch A was purified to homogeneity by semi-preparative C_{18} reverse-phase HPLC, as described in experimental procedures. In analytical reverse phase HPLC conditions, the purified synthetic Aah I [sAah I, Fig. 2(c)] was eluted at a retention time similar to that for natural Aah I [Fig. 2(d)]. When injected together, sAah I and natural Aah I (4.5 nmol of each) were indistinguishable in terms of HPLC elution [Fig. 2(e)] and MS analysis [Fig. 2(f)]. Indeed, the experimental mass M_r $(M + H)^+$ of sAah I obtained by MALDI-TOF I was

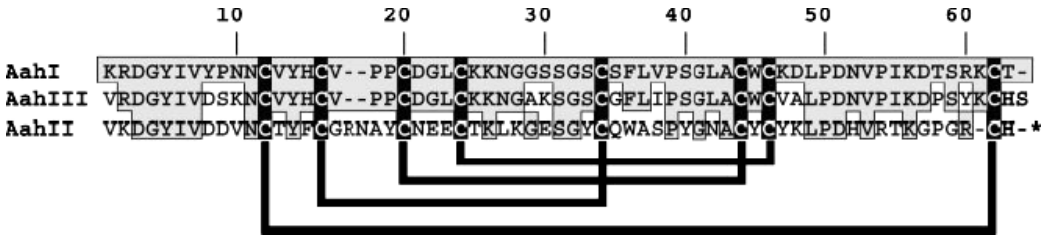

Figure 1 Amino-acid sequence (one-letter code) of Aah I and comparison with the related scorpion toxin sequences Aah II and Aah III. The amino-acid sequences of Aah I [64], Aah II [65] and Aah III [66] from *Androctonus australis hector* were aligned on the basis of half-cystine residues. Gaps (–) were introduced in the amino-acid sequences to maximize homology. The positions of half-cystines are indicated in black boxes and amino acid residues are numbered. Amino-acid sequence identities are boxed in grey. Asterisks indicate an amidated C-terminal.

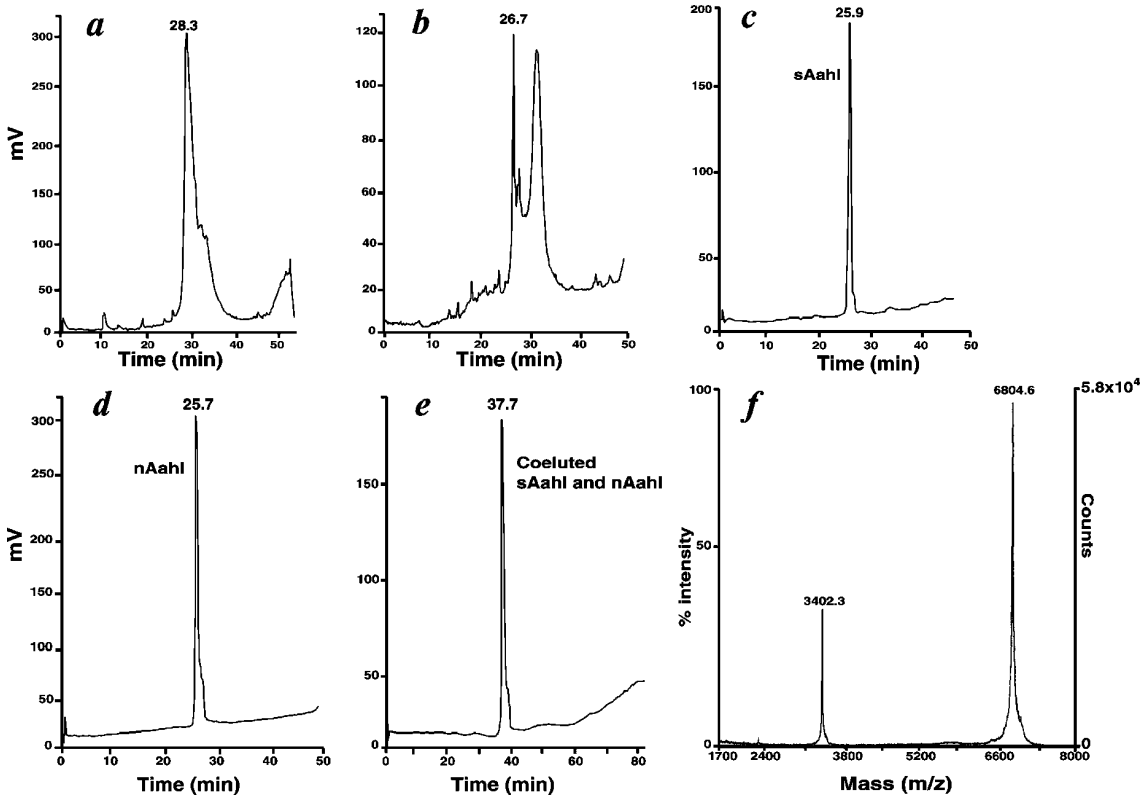

Figure 2 Analytical C_{18} RP-HPLC profiles of synthetic Aah I at various stages of peptide synthesis. (a) Crude reduced peptide after trifluoroacetic acid cleavage. (b) Crude peptide after 160 h of folding/oxidation. (c) and (d) Purified folded sAah I (9 nmol) and natural Aah I (11 nmol), respectively. For (a)–(d), conditions were: 40 min linear gradient from 0 to 60% of buffer B [0.08% (v/v) TFA-acetonitrile] in buffer A [0.1% (v/v) TFA-H_2O], 1 ml/min. (e) Co-elution of 4.5 nmol of sAah I with 4.5 nmol of natural Aah I. Conditions were: 60 min linear gradient from 0 to 60% of buffer B [0.08% (v/v) TFA-acetonitrile] in buffer A [0.1% (v/v) TFA-H_2O], 1 ml/min. (f) MALDI-TOF mass spectrum of the unique peak collected from co-elution HPLC. m/z is the ratio of molecular mass to the number of charges of the ionized species.

6804.5, which is very close to both the theoretical mass (6804.9 Da), and the experimental mass of natural Aah I: $(M + H)^+ = 6804.8$ Da. Amino-acid analyses of dried sAah I showed that its net peptide content was 80% (w/w), and that its amino-acid composition was consistent with the theoretical composition (not shown). Edman degradation of reduced and carboxamidomethylated sAah I (batch B) was performed until residue 27. After correction for background, it was estimated that 9% of peptide presented one deletion occurring in the 27 first residues. The final amount of sAah I was 150 μg (22 nmol) for batch A and 500 μg (73 nmol) for batch B.

The CD spectra of natural and synthetic AahI were recorded to assess their secondary structures (Fig. 3). Measurements were performed at a wavelength ranging from 190 to 260 nm. The data obtained correspond essentially to π–π^* and n–π^* transitions of the amide chromophores of the peptide backbones [67]. The CD spectra of natural and synthetic Aah I look very similar and show large negative contributions between 207 and 230 nm, and large positive contributions between 190 and 200 nm, indicating the presence of both α-helical and β-sheet structures. These data are coherent with a peptide backbone folding according to an α/β scaffold [68] for both nAahI and sAahI.

Comparative Biological Assays

Electrophysiological assays. By voltage-clamp experiments, we compared the functional effects of native and synthetic Aah I molecules on $Na_v1.2$ NaChs expressed transiently in tsA-201 cells. Figure 4(a) shows the membrane sodium currents obtained in response to a step depolarization from a holding potential of −120 mV to a membrane potential of −10 mV. In control conditions, complete sodium current inactivation occurred in 2 ms.

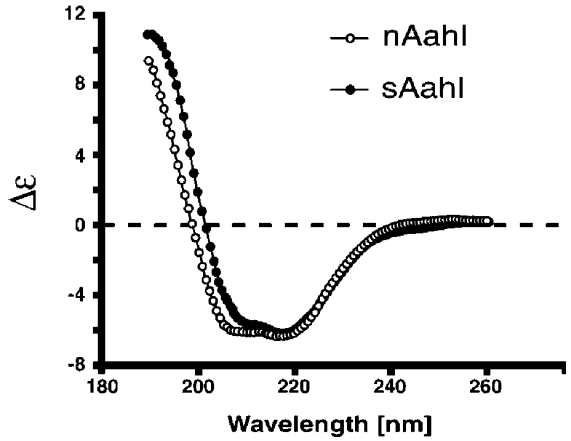

Figure 3 CD spectra of 0.1 mg/ml solutions of natural (open circles) and synthetic (solid circles) Aah I toxins. Spectra were recorded between 190 and 260 nm, in a 0.1 cm path length quartz cell, at 20 °C. The measure is reported as the absorption coefficient ($\Delta\varepsilon$) per amide.

In contrast, in the presence of saturating concentrations of both natural (0.553 μM) and synthetic (1.22 μM) Aah I, up to 60% of the current remained after 2 ms [Fig. 4(a)]. Thus, although tested at a different concentration, sAah I inhibits NaChs inactivation similarly to the natural toxin. To reliably compare the K_d of the natural and synthetic toxins for $Na_v1.2$ NaChs, we carried out the same experiment in the presence of a lower concentration of toxin. The fraction of conductance remaining 2 ms after the peak was found to be proportional to the number of channels modified by α-scorpion toxin. This fraction can be used to estimate receptor occupancy and toxin affinity as follows:

$$K_d = \frac{[\text{ScTox}]}{(F'_G/F_G - 1)}$$

where [ScTox] is the toxin concentration, F_G is the fraction of sodium current remaining 2 ms after the beginning of the pulse, and F'_G is the maximum fraction of current 2 ms after the beginning of the pulse in the presence of a saturating concentration of α-scorpion toxin. This gave a K_d of 6.1 ± 0.07 nM ($n = 8$) for the natural toxin and of 15.1 ± 0.1 nM ($n = 9$) for the synthetic toxin. Analysis of conductance/voltage relationships in the presence and absence of natural or synthetic toxins revealed that both molecules shifted the voltage-dependence of activation to more positive potentials [Fig. 4(b)], while they shifted the inactivation curve by 17 mV towards positive potentials [Fig. 4(c)]. Thus, electrophysiological properties of the channels are modified by natural and synthetic Aah I similarly.

***In vivo* toxicity assays.** We compared the toxicity of natural and synthetic Aah I *in vivo* following i.c.v. injections in C57BL/6 mice. We obtained LD_{50} values of 9 and 13 ng per 20 g mouse for natural Aah I and sAah I, respectively. The symptoms observed in mice injected with sAah I were typical of those induced by α-toxins, and were similar to those induced by natural Aah I, used as a control.

Immunological assays (RIA). Monoclonal and polyclonal anti-Aah I antibodies were used to compare, in RIA, the antigenic properties of sAah I and natural Aah I. The sAah I molecule outcompeted [^{125}I]-labelled natural Aah I for binding to the conformation-dependent mAb 9C2. We found that sAah I completely inhibited [^{125}I]-Aah I binding to 9C2, with an IC_{50} of 0.67 ± 0.24 nM [Fig. 5(a)]. Unlabelled natural Aah I was tested over a similar concentration range and inhibited the binding of [^{125}I]-Aah I to 9C2 with an IC_{50} of 0.44 ± 0.16 nM. The inhibition curve in Fig. 5(b) shows the ability of sAah I to compete with [^{125}I]-Aah I for binding to the P111 anti-Aah I polyclonal Ab obtained from rabbit. The sAah I toxin was recognized by P111 Ab with an IC_{50} value of 1.48 ± 0.3 nM, whereas the IC_{50} value was 0.68 ± 0.1 nM for the natural Aah I.

DISCUSSION

The North-African *Buthidae* scorpion *Androctonus australis hector* is probably the most dangerous scorpion as regards the severity of envenomation. Its venom principally contains three mammal-selective neurotoxins: the well-studied Aah II toxin, and its two most important companion toxins, Aah I and Aah III. Whereas research in mammal-selective scorpion α-toxins has focused almost exclusively on Aah II until now, the study of Aah I or Aah III toxins has been more or less neglected, although both are also effective modifiers of NaChs. Actually, although 20 times less toxic than Aah II by i.c.v. route [37], Aah I has almost the same lethal potency by peripheral inoculation. As such, Aah I should be neutralized as efficiently as Aah II in the treatment of envenomations due to *Androctonus australis hector* scorpions.

In previous works, attempts to obtain the *Tityus serrulatus* toxin 7 (Ts 7) or Aah II by chemical synthesis or molecular biology resulted in very

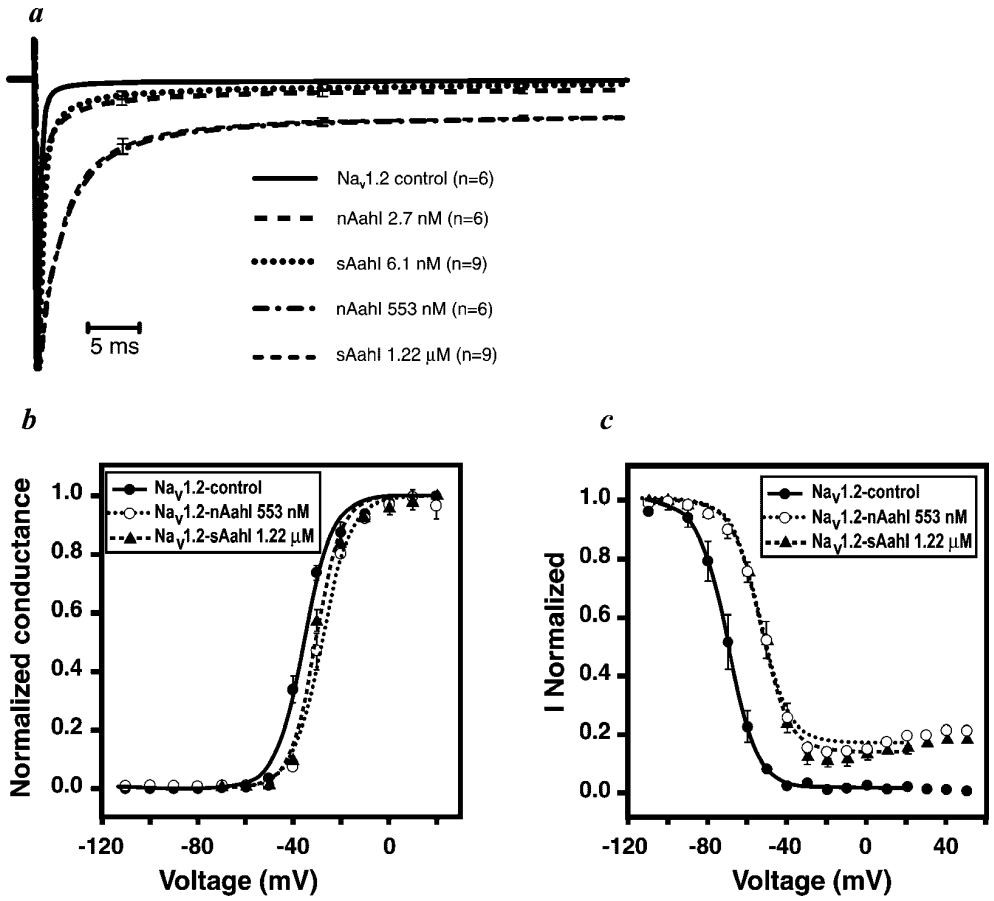

Figure 4 Electrophysiological effect of natural and synthetic Aah I on Na$_v$1.2 NaChs. (a) Sodium currents elicited by step-wise depolarization to −10 mV in control conditions or in the presence of various concentrations of natural or synthetic Aah I toxins. (b) Effects of natural and synthetic Aah I on NaCh activation. Sodium peak currents were recorded during voltage pulses from −110 to +130 mV for 30 ms. Conductance-voltage curves were derived from peak sodium current vs voltage measurements according to the relationship $G = I/(V - V_R)$ where I is the peak current, V is the test voltage, and V_R is the apparent reversal potential. Normalized voltage-conductance curves were fitted with a Boltzman relationship. (c) Voltage dependence of inactivation. Inactivation curves were determined using a 100 ms prepulse to the indicated potentials, followed by test pulses to −10 mV in control conditions or in the presence of toxins. Normalized current-voltage curves were fitted with a single Boltzman relationship.

low yields, with no complete physicochemical or biological characterizations [43,54]. We often observed that Aah I was more soluble and stable in solution than Aah II or Ts 7, and this would have made Aah I easier to handle and convinced us to undertake its chemical synthesis.

Aah I has six proline residues, with a Pro — Pro sequence in positions 18–19. It lacks Met, Glu and Gln residues and its C-terminal end is a carboxylate [64]. After Aah I assembly completion, we could expect a mass increase of about 3.62 g for 0.3 mmol of peptidyl-resin. Actually, we obtained about 3.1 g (74%), which indicates that some problems occurred during the assembly process. This was confirmed since MS revealed that truncated peptides were present in the crude peptide fraction as well as in the precipitate that formed during oxidation. The folding/oxidation experiments were carried out under concentrated peptide conditions, since we observed previously that they could favour precipitation, hence elimination, of truncated peptides or peptides with scrambled disulphides during oxidation/folding of K^+ channel-selective 'short neurotoxins'. The precipitate that occurred during oxidation was partially re-dissolved in DMSO. By MS, it revealed only a minor amount of oxidized sAahI, but a well-populated family of shortened peptides with molecular mass values under 4000 Da, which indicated that most of the truncated peptides aggregated and eventually precipitated.

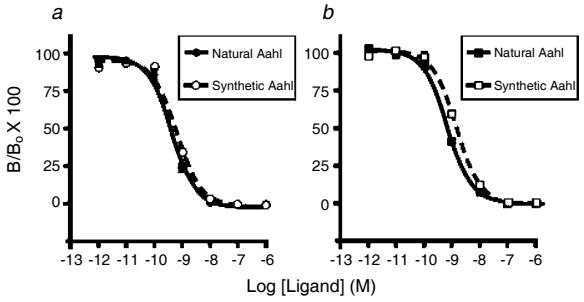

Figure 5 Recognition of natural and synthetic Aah I by anti-Aah I mAb 9C2 and pAb P111, based on binding to [^{125}I]Aah I in competitive RIA. Immuno-reactivity of (a) mAb 9C2, and (b) pAb 111 with natural (solid symbols) and synthetic (open symbols) Aah I. *B* and B_0 are the radioactivity bound to antibody in the presence *(B)* and absence (B_0) of unlabelled ligand respectively. Error bars are shown; if not visible, this is because they fall within the bounds of the symbol.

After purification, sAah I was characterized and compared with natural AahI in several ways. A strange feature of sAah I was that it eluted not only as a main peak in reverse-phase HPLC, but it showed also two smaller peaks or 'shoulders', all three with the same molecular mass [see the main peak tails in Fig. 2(c)–(e)]. In fact, we observed similar profiles with the natural Aah I toxin in the same HPLC conditions (unpublished results). Moreover, when rechromatographed in the same conditions, any each of the three previously isolated peaks gave the same original pattern, with similar relative amounts of products with the theoretical mass of the toxin (not shown). We made the assumption that natural Aah I may exist as three distinct conformers, and that the preparation of samples before chromatography probably results in a new equilibrium between these conformers. This phenomenon has yet been described for synthetic proline-rich peptides, due to *cis*-/*trans*-proline exchange of peptide bonds [69]. Thus, the observed multi-bumped HPLC profile of the synthetic product was considered to provide an additional evidence of its equivalence to the natural molecule.

We obtained about 150 μg (0.38%) of active toxin from 40 mg of crude peptide in one oxidation/folding experiment (batch A), and 500 μg (2%) from 25 mg in the other (batch B). Considering that the most productive experiment gave a 2% toxin yield, and that we could expect 1.29 g of crude peptide from the total amount of peptidyl-resin, it seems reasonable to count on a final amount of about 26 mg (3.8 μmol) of sAah I. This may appear as low, but the overall conditions of assembly and oxidation have not yet been optimized. After analysis of the truncated peptides, we could probably identify the assembly steps that produced a partial blockage of the coupling reaction, and we may therefore optimize the coupling conditions. Also, both the DMSO and crude peptide concentrations could be adjusted to increase the fraction of correctly folded toxin in solution. We did not renaturate sAah I in presence of oxidized/reduced glutathion since, in previous attempts at synthesizing other long toxins, we observed unexpectedly that such conditions produced non-native molecules with scrambled disulphides, and also favoured the formation of stable derivatives with intermolecular toxin-glutathion bridges.

Overall, the biochemical and physicochemical properties of sAahI (amino-acid composition and sequence, molecular mass. HPLC retention time, CD spectra and conformer equilibrium) testified to a biochemical identity with its natural model. Moreover, biological tests showed that the purified oxidized/folded Aah I behaved similarly to nAah I. Toxicity determination has been considered as one of the best tests for monitoring toxin reoxidation — renaturation [53]. Indeed, the i.c.v. injection of sAah I into mice produced immediate toxic symptoms, identical to those observed on control animals injected with natural Aah I, and characteristic of α-toxins, suggesting that inhibition of the NaCh inactivation was the actual effect of the synthetic product at a molecular level. This was confirmed by voltage-clamp experiments, that showed that both the synthetic and natural Aah I toxins inhibited NaCh inactivation similarly. Thus, it was established that all pharmacological effects of sAah I are characteristic of α-type toxins and very closely resemble those of natural Aah I.

Unlike neurotoxicity, the immunological properties of toxins are not so much susceptible to conformational deviations, but specific anti-toxin antibodies that recognize conformational epitopes may indicate the level of structural conformity between a natural toxin and its synthetic replica. The 9C2 mAb that we used in our tests is likely to be conformation-dependent, since its binding to natural [^{125}I]-Aah I was not prevented by Abu 8 Aah I, a synthetic, incompletely structured Aah I analogue with all half-cystines replaced by α-aminobutyric acid [59]. Indeed, sAah I completely inhibited the binding of [^{125}I]-Aah I to monoclonal or polyclonal anti-Aah I antibodies, with IC_{50} values in a range similar to those for the natural toxin. The good reactivity of pAb

111 polyclonal antibodies towards sAah I indicates that it displays the same epitopes as the natural toxin but more importantly, the high reactivity of the 9C2 anti-Aah I monoclonal antibody indicates that it recognizes the same conformational epitope on both the natural and synthetic toxins.

In conclusion, we found synthesis and folding conditions suitable for obtaining enough synthetic Aah I toxin for pharmacological or immunological purposes. We could reasonably expect to obtain the toxin in centigram amounts, which is particularly important given the scarcity and high cost of the natural toxin. In our knowledge, this is the first successful chemical synthesis of a NaCh-selective scorpion neurotoxin. This work may be followed by chemical synthesis of variants or modified derivatives of Aah I, such as artificial point mutants or engineered anatoxins. Our results may also open a way for synthesizing other pharmacologically important long-chain neurotoxins and targeted engineered mutants. The solid-phase chemical synthesis of neurotoxins thus appears as complementary to recombinant expression techniques and could offer the possibility of engineering more diversely modified molecules.

Acknowledgements

We thank Dr Christian Cambillau for providing facilities of using the CD spectrometer. We would like to thank Dr Marie-France Martin-Eauclaire for providing purified natural scorpion neurotoxins. The French CNRS, the Université de la Méditerranée, and Cellpep S.A. provided financial support for this study.

REFERENCES

1. Goyffon M, Vachon M, Broglio N. Epidemiological and clinical characteristics of the scorpion envenomation in Tunisia. *Toxicon* 1982; **20**: 337–344.
2. Ismail M. The scorpion envenoming syndrome. *Toxicon* 1995; **33**: 825–858.
3. Miranda F, Rochat H, Rochat C, Lissitzky S. Molecular complexes present in animal neurotoxins. 1. Neurotoxins of venoms of scorpions *Androctonus australis Hector* and *Buthus occitanus tunetanus*. *Toxicon* 1966; **42**: 123–144.
4. Carbone E, Wanke E, Prestipino G, Possani LD, Maelicke A. Selective blockage of voltage-dependent K^+ channels by a novel scorpion toxin. *Nature (Lond.)* 1982; **296**: 90–91.
5. Crest M, Jacquet G, Gola M, Zerrouk H, Benslimane A, Rochat H, Mansuelle P, Martin-Eauclaire M-F. Kaliotoxin, a novel peptidyl inhibitor of neuronal BK-type $Ca^{(2+)}$-activated K^+ channels characterized from *Androctonus mauretanicus mauretanicus* venom. *J. Biol. Chem.* 1992; **267**: 1640–1647.
6. Rochat H, Bernard P, Couraud F. *Advances in Cytopharmacology*, Cecarelli B, Clementi F (eds), Vol. 3. Raven Press: New York; 325–334.
7. Possani LD, Becerril B, Delepierre M. Tytgat J. Scorpion specific for Na^+ channels. *Eur. J. Biochem.* 1999; **264**: 287–300.
8. Zlotkin E, Rochat H, Kopeyan C, Miranda F, Lissitzky S. Purification and properties of the insect toxin from the venom of the scorpion *Androctonus australis Hector*. *Biochimie* 1971; **53**: 1073–1078.
9. Loret EP, Mansuelle P, Rochat H, Granier C. Neurotoxins active on insects: amino acid sequences, chemical modifications, and secondary structure estimation by circular dichroism of toxins from the scorpion *Androctonus australis Hector*. *Biochemistry* 1990; **29**: 1492–1501.
10. Zlotkin E, Gurevitz M, Fowler E, Adams ME. Depressant insect selective neurotoxins from scorpion venom: chemistry, action, and gene cloning. *Arch Insect Biochem Physiol.* 1993; **22**: 55–73.
11. Cestèle S, Kopeyan C, Oughideni R, Mansuelle P, Granier C, Rochat H. Biochemical and pharmacological characterization of a depressant insect toxin from the venom of the scorpion *Buthacus arenicola*. *Eur. J. Biochem.* 1997; **243**: 93–99.
12. Zlotkin E, Miranda F, Lissitzky S. A factor toxic to crustaceans in the venom of the scorpion *Androctonus australis Hector*. *Toxicon* 1972; **10**: 211–216.
13. Lebreton F, Delepierre M, Ramirez AN, Balderas C, Possani LD. Primary and NMR three-dimensional structure determination of a novel crustacean toxin from the venom of the scorpion *Centruroides limpidus limpidus* Karsch. *Biochemistry* 1994; **33**: 11 135–11 149.
14. De Lima ME, Martin MF, Diniz CR, Rochat H. *Tityus serrulatus* toxin VII bears pharmacological properties of both beta-toxin and insect toxin from scorpion venoms. *Biochem. Biophys. Res. Commun.* 1986; **29**: 296–302.
15. Kopeyan C, Mansuelle P, Martin-Eauclaire MF, Rochat H, Miranda F. Characterization of toxin III of the scorpion *Leiurus quinquestriatus quinquestriatus*: a new type of alpha-toxin highly toxic both to mammals and insects. *Nat. Toxins* 1993; **1**: 308–312.
16. Chejanovsky N, Zilberberg N, Rivkin H, Zlotkin E, Gurevitz M. Functional expression of an alpha anti-insect scorpion neurotoxin in insect cells and lepidopterous larvae. *FEBS Lett.* 1995; **376**: 181–184.
17. Gordon D, Martin-Eauclaire MF, Cestèle S, Kopeyan C, Carlier E, Ben Khalifa R, Pelhate M, Rochat H. Scorpion toxin affecting sodium current inactivation bind to distinct homologous receptor sites on rat brain

and insect sodium channels. *J. Biol. Chem.* 1996; **271**: 8034–8054.
18. Jover E, Couraud F, Rochat H. Two types of scorpion neurotoxins characterized by their binding to two separate receptor sites on rat brain synaptosomes. *Biochem. Biophys. Res. Commun.* 1980; **95**: 1607–1614.
19. Couraud F, Jover E, Dubois JM, Rochat H. Two types of scorpion toxin receptor sites, one related to the activation, the other to the inactivation of the action potential sodium channel. *Toxicon* 1982; **20**: 9–16.
20. Gordon D, Savarin P, Gurevitz M, Zinn-Justin S. Functional anatomy of scorpion toxins affecting sodium channels. *J. Toxicol. Toxin. Rev.* 1998; **7**: 131–158.
21. Gilles N, Blanchet C, Shichor I, Zaninetti M, Lotan I, Bertrand D, Gordon D. A scorpion α-like toxin that is active on insects and mammals reveals an unexpected specificity and distribution of sodium channels subtypes in rat brain neurons. *J. Neurosci.* 1999; **19**: 8730–8739.
22. Miranda F, Kupeyan C, Rochat H, Rochat C, Lissitzky S. Purification of animal neurotoxins: isolation and characterization of eleven neurotoxins from the venoms of the scorpions *Androctonus australis Hector*, *Buthus occitanus tunetanus* and *Leiurus quinquestriatus quinquestriatus*. *Eur. J. Biochem.* 1970; **16**: 514–523.
23. Jover E, Martin-Moutot N, Couraud F, Rochat H. Binding of scorpion toxins to rat brain synaptosomal fraction. Effects of membrane potential, ion, and other neurotoxins. *Biochemistry* 1980; **19**: 463–467.
24. Catterall WA. Molecular properties of voltage-sensitive sodium channels. *A Rev. Biochem.* 1986; **55**: 953–985.
25. Catterall WA. Cellular and molecular biology of voltage-gated sodium channels. *Physiol. Rev.* 1992; **72**: 15–48.
26. Rogers JC, Qu Y, Tanada TN, Scheuer T, Catterall WA. Molecular determinants of high affinity binding of α-scorpion toxin and sea anemone toxin in the S3-S4 extracellular loop in domain IV of the Na^+ channel α-subunit. *J. Biol. Chem.* 1996; **271**: 15 950–15 962.
27. Fontecilla-Camps JC, Almassy RJ, Suddath FL, Watt DD, Bugg CE. Three dimensional structure of a protein from scorpion venom: a new structural class of neurotoxins. *Proc. Natl. Acad. Sci. USA* 1980; **77**: 6496–6500.
28. Housset D, Habersetzer-Rochat C, Astier JP, Fontecilla-Camps JC. Crystal structure of toxin II from the scorpion *Androctonus australis Hector* refined at 1.3 Å resolution. *J. Mol. Biol.* 1994; **238**: 88–103.
29. Tugarinov V, Kustanovich I, Zilberberg N, Gurevitz M, Anglister J. Solution structures of a highly insecticidial recombinant scorpion α-toxin and a mutant with increased activity. *Biochemistry* 1997; **36**: 2414–2424.
30. Polikarpov I, Junior MS, Marangoni S, Toyama MH, Teplyakov A. Crystal structure of neurotoxin Ts1 from *Tityus serrulatus* provides insights into the specificity and toxicity of scorpion toxins. *J. Mol. Biol.* 1999; **290**: 175–184.
31. He XL, Li HM, Zeng ZH, Liu XQ, Wang M, Wang DC. Crystal structures of two alpha-like scorpion toxins: non-proline *cis* peptide bonds and implications for new binding site selectivity on the sodium channel. *J. Mol. Biol.* 1999; **292**: 125–135.
32. Oren DA, Froy O, Amit E, Kleinberger-Doron N, Gurevitz M, Shaanan B. An excitatory scorpion toxin with a distinctive feature: an additional alpha helix at the C terminus and its implications for interaction with insect sodium channels. *Structure* 1998; **6**: 1095–1103.
33. Sampieri F. Habersetzer-Rochat C. Structure-function relationships in scorpion neurotoxins: identification of the superreactive lysine residue in toxin I of *Androctonus australis Hector*. *Biochim. Biophys. Acta* 1978; **535**: 100–109.
34. Darbon H, Jover E, Couraud F, Rochat H. α-Scorpion neurotoxin derivatives suitable as potential markers of sodium channels. *Int. J. Peptide Protein Res.* 1983; **22**: 179–186.
35. Kharrat R, Darbon H, Rochat H, Granier C. Structure/activity relationships of scorpion α-toxins. Multiple residues contribute to the interaction with receptors. *Eur. J. Biochem.* 1989; **181**: 381–390.
36. Hassani O, Mansuelle P, Cestèle S, Bourdeaux M, Rochat H, Sampieri F. Role of lysine and tryptophan residues in the biological activity of toxin VII (Ts gamma) from the scorpion *Tityus serrulatus*. *Eur. J. Biochem.* 1999; **260**: 76–86.
37. Martin MF, Rochat H. Large-scale purification of toxins from the venom of the scorpion *Androctonus australis hector*. *Toxicon* 1986; **24**: 1131–1139.
38. Zilberberg N, Gordon D, Pelhate M, Adams ME, Norris TM, Zlotkin E, Gurevitz M. Functional expression and genetic alteration of an alpha scorpion neurotoxin. *Biochemistry* 1996; **35**: 10 215–10 222.
39. Zilberberg N, Froy O, Loret E, Cestèle S, Arad D, Gordon D, Gurevitz M. Identification of structural elements of a scorpion α-neurotoxin important for receptor site recognition. *J. Biol. Chem.* 1997; **272**: 14 810–14 816.
40. Froy O, Zilberberg N, Gordon D, Turkov M, Gilles N, Stankiewicz M, Pelhate M, Loret E, Oren DA, Shaanan B, Gurevitz M. The putative bioactive surface of insect-selective scorpion excitatory neurotoxins. *J. Biol. Chem.* 1999; **274**: 5769–5776.
41. Shao F, Xiong YM, Zhu RH, Ling MH, Chi CW, Wang DC. Expression and purification of the BmK M1 neurotoxin from the scorpion *Buthus martensi* Karsch. *Protein Expr. Purif.* 1999; **17**: 358–365.
42. Sun YM, Liu W, Zhu RH, Goudet C, Tytgat J, Wang DC. Role of disulfide bridges in scorpion toxin BmK M1 analyzed by mutagenesis. *J. Pept. Res.* 2002; **60**: 247–256.
43. Bougis PE, Rochat H, Smith LA. Precursors of *Androctonus australis* scorpion neurotoxins. Structures of

precursors, processing outcomes, and expression of a functional recombinant toxin II. *J. Biol. Chem.* 1989; **264**: 19 259–19 265.
44. Martin-Eauclaire M-F, Sogaard M, Ramos C, Cestèle S, Bougis PE, Svensson B. Production of active, insect-specific scorpion neurotoxin in yeast. *Eur. J. Biochem.* 1994; **233**: 637–645.
45. Devaux C, Clot-Faybesse O, Juin M, Mabrouk K, Sabatier JM, Rochat H. Monoclonal antibodies neutralizing the toxin II from *Androctonus australis hector* scorpion venom: usefulness of a synthetic, non-toxic analog. *FEBS Lett.* 1997; **412**: 456–460.
46. Zhu Q, Liang S, Martin L, Gasparini S, Ménez A, Vita C. Role of disulfide bonds in folding and activity of leiurotoxin I: just two disulfides suffice. *Biochemistry* 2002; **41**: 11 488–11 494.
47. Giangiacomo KM, Sugg EE, Garcia-Calvo M, Leonard RJ, McManus OB, Kaczorowski GJ, Garcia ML. Synthetic charybdotoxin-iberiotoxin chimeric peptides define toxin binding sites on calcium-activated and voltage-dependent potassium channels. *Biochemistry* 1993; **32**: 2363–2370.
48. Romi R, Crest M, Gola M, Sampieri F, Jacquet G, Zerrouk H, Mansuelle P, Sorokine O, Van Dorsselaer A, Rochat H, Martin-Eauclaire M-F, Van Rietschoten J. Synthesis and characterization of kaliotoxin. Is the 26–32 sequence essential for potassium channel recognition? *J. Biol. Chem.* 1993; **268**: 26 302–26 309.
49. Sabatier JM, Femont V, Mabrouk K, Crest M, Darbon H, Rochat H, Van Rietschoten J, Martin-Eauclaire MF. Leiurotoxin I, a scorpion toxin specific for Ca^{2+}-activated potassium channels: structure activity relationships using synthetic analogs. *Int. J. Peptide Protein Res.* 1994; **43**: 486–495.
50. Bednarek MA, Bugianesi RM, Leonard RJ, Felix JP. Chemical synthesis and structure-function studies of margatoxin, a potent inhibitor of voltage-dependent potassium channel in human T lymphocytes. *Biochem. Biophys. Res. Commun.* 1994; **198**: 619–625.
51. Kharrat R, Mabrouk K, Crest M, Darbon H, Oughideni R, Martin-Eauclaire MF, Jacquet G, El Ayeb M, Van Rietschoten J, Rochat H, Sabatier JM. Chemical synthesis and characterization of maurotoxin, a short scorpion toxin with four disulfide bridges that acts on K^+ channels. *Eur. J. Biochem.* 1996; **242**: 491–498.
52. Torres AM, Bansal P, Alewood PF, Bursill JA, Kuchel PW, Vandenberg JI. Solution structure of CnErg1 (Ergtoxin), a HERG specific scorpion toxin. *FEBS Lett.* 2003; **539**: 138–142.
53. Sabatier JM, Darbon H, Fourquet P, Rochat H, Van Rietschoten J. Reduction and reoxidation of the neurotoxin II from the scorpion *Androctonus australis Hector*. *Int. J. Pept. Protein Res.* 1987; **30**: 125–134.
54. Romi R. La synthèse peptidique en phase solide appliquée aux neurotoxins de scorpions: assemblage et renaturation de la toxine VII de *Tityus serrulatus*; études des relations structure-activité de la kaliotoxine d'*Androctonus mauretanicus mauretanicus*. PhD thesis, Université de Provence.
55. Merrifield RB. Solid-phase synthesis. *Science* 1986; **232**: 341–347.
56. Wang SS. p-Alkoxybenzyl alcohol resin and p-alkoxybenzyloxycarbonyl-hydrazide resin for solid phase synthesis of protected peptide fragments. *J. Am. Chem. Soc.* 1973; **95**: 1328–1333.
57. Sieber P. An improved method for anchoring of 9-fluorenylmethyloxycarbonyl-amino acids to 4-alkoxybenzyl alcohol resins. *Tetrahedron Lett.* 1987; **28**: 6147–6150.
58. Niall HD, Tregear GW, Jacobs J. *Chemistry and Biology of Peptides*, Meienhofer J (ed.). Ann Arbor Science: Ann Arbor MI, 695–699.
59. Clot-Faybesse O, Juin M, Rochat H, Devaux C. Monoclonal antibodies against the *Androctonus australis hector* scorpion neurotoxin I: characterisation and use for venom neutralisation. *FEBS Lett.* 1999; **458**: 313–318.
60. Delori P, Van Rietschoten J, Rochat H. Scorpion venoms and neurotoxins: an immunological study. *Toxicon* 1981; **19**: 393–407.
61. Rochat H, Tessier M, Miranda F, Lissitzky S. Radioiodination of scorpion and snake toxins. *Anal. Biochem.* 1977; **82**: 532–548.
62. Behrens B, Karber G. Wie sind Reihenversuche für biologische Auswertungen am zweckmässigsten anzuorden. *Arch. Exp. Pathol. Pharmak.* 1935; **177**: 379–388.
63. Jordan M, Schallhorn A, Wurm FM. Transfecting mammalian cells: optimization of critical parameters affecting calcium-phosphate precipitate formation. *Nucl Acids Res.* 1996; **15**: 596–601.
64. Rochat H, Rochat C, Miranda F, Lissitzky S, Edman P. The amino acid sequence of neurotoxin I of *Androctonus australis Hector*. *Eur. J. Biochem.* 1970; **17**: 262–266.
65. Rochat H, Rochat C, Sampieri F, Miranda F, Lissitzky S. The amino-acid sequence of neurotoxin II of *Androctonus australis Hector*. *Eur. J. Biochem.* 1972; **28**: 381–388.
66. Kopeyan C, Martinez G, Rochat H. Amino acid sequence of neurotoxin III of the scorpion *Androctonus australis Hector*. *Eur J. Biochem.* 1979; **94**: 609–615.
67. Johnson WC. Circular dichroism and its empirical application to biopolymers. *Meth. Biochem. Anal.* 1985; **31**: 61–163.
68. Bontems F, Roumestand C, Gilquin B, Ménez A, Toma F. Refined structure of charybdotoxin: common motifs in scorpion toxins and insect defensins. *Science* 1991; **254**: 1521–1523.
69. O'Neal KD, Chari MV, McDonald CH, Cook RG, Yu-Lee LY, Morriss JD, Shearer WT. Multiple *cis-trans* conformers of the prolactin receptor proline-rich motif (PMR) peptide detected by reverse-phase HPLC, CD and NMR spectroscopy. *Biochem. J.* 1996; **315**: 833–844.

